



Rapid Prototyping Journal

Selective laser melting of Ti6Al7Nb with hydroxyapatite addition

Teodora Marcu, Cinzia Menapace, Luca Girardini, Dan Leordean, Catalin Popa,

Article information:

To cite this document:

Teodora Marcu, Cinzia Menapace, Luca Girardini, Dan Leordean, Catalin Popa, (2014) "Selective laser melting of Ti6Al7Nb with hydroxyapatite addition", Rapid Prototyping Journal, Vol. 20 Issue: 4, pp.301-310, doi: 10.1108/RPJ-09-2012-0083

Permanent link to this document:

<http://dx.doi.org/10.1108/RPJ-09-2012-0083>

Downloaded on: 18 May 2017, At: 02:41 (PT)

References: this document contains references to 13 other documents.

To copy this document: permissions@emeraldinsight.com

The fulltext of this document has been downloaded 266 times since 2014*

Users who downloaded this article also downloaded:

(2015), "Customized implants with specific properties, made by selective laser melting", Rapid Prototyping Journal, Vol. 21 Iss 1 pp. 98-104 <http://dx.doi.org/10.1108/RPJ-11-2012-0107>

(2014), "Selective laser melting (SLM) of pure gold for manufacturing dental crowns", Rapid Prototyping Journal, Vol. 20 Iss 6 pp. 471-479 <http://dx.doi.org/10.1108/RPJ-03-2013-0034>

Access to this document was granted through an Emerald subscription provided by emerald-srm:313859 []

For Authors

If you would like to write for this, or any other Emerald publication, then please use our Emerald for Authors service information about how to choose which publication to write for and submission guidelines are available for all. Please visit www.emeraldinsight.com/authors for more information.

About Emerald www.emeraldinsight.com

Emerald is a global publisher linking research and practice to the benefit of society. The company manages a portfolio of more than 290 journals and over 2,350 books and book series volumes, as well as providing an extensive range of online products and additional customer resources and services.

Emerald is both COUNTER 4 and TRANSFER compliant. The organization is a partner of the Committee on Publication Ethics (COPE) and also works with Portico and the LOCKSS initiative for digital archive preservation.

*Related content and download information correct at time of download.

Selective laser melting of Ti6Al7Nb with hydroxyapatite addition

Teodora Marcu

Department of Materials Science and Technology, Technical University of Cluj-Napoca, Cluj-Napoca, Romania

Cinzia Menapace

Department of Materials Engineering and Industrial Technologies, University of Trento, Trento, Italy

Luca Girardini

K4Sint S.r.l., Pergine Valsugana (TN), Italy

Dan Leordean

Department of Manufacturing Technology, Technical University of Cluj-Napoca, Cluj-Napoca, Romania, and

Catalin Popa

Department of Materials Science and Technology, Technical University of Cluj-Napoca, Cluj-Napoca, Romania

Abstract

Purpose – The purpose of this paper was to obtain by means of selective laser melting and then characterize biocomposites of medical-grade Ti6Al7Nb with hydroxyapatite (2 and 5 vol.%) and without hydroxyapatite, as reference.

Design/methodology/approach – Rectangular samples were manufactured with the same scanning strategy; the laser power was between 50 W and 200 W. Processed samples were analysed by means of optical microscopy, scanning electron microscopy and microhardness.

Findings – The results showed that despite the very short processing times, hydroxyapatite decomposed and interacted with the base Ti6Al7Nb material. The decomposition degree was found to depend on the applied laser power. From the porosity and bulk microstructure point of view, the most appropriate materials for the purposed medical applications were Ti6Al7Nb with hydroxyapatite processed with a laser power of 50 W.

Originality/value – The originality of the present work consists in the study of the behaviour and interaction of hydroxyapatite additive with the Ti6Al7Nb base powder under selective laser melting conditions, as depending on the applied laser power.

Keywords Selective laser melting, Titanium alloy, Hydroxyapatite, Hydroxyapatite decomposition, Microstructure

Paper type Research paper

1. Introduction

Additive manufacturing methods are often used for biomedical applications due to their capability to create a personalized implant design based on a CAD model, with a designed and well-controlled porosity (Bremen *et al.*, 2012). Although applied to a large variety of powders, the metallurgical behaviour of the processed materials have not been well-understood (Simchi, 2006).

Porous Ti-based structures received an increased consideration in the medical field, for endosseous implants, due to their lower elastic modulus if compared to bulk Ti and, consequently, to their lower tendency towards the stress-shielding phenomenon (Sobieszczyk, 2010). To improve the bioactivity and osseointegration of these structures, hydroxyapatite (HA) is often used, in addition to the base material. Although the biocompatibility of porous

Ti-HA composites is well-assessed (Balbinotti *et al.*, 2011; Ning *et al.*, 2002), the bioactivity of future implant depends on the surface chemistry, as resulting from the decomposition of HA and subsequent interaction with Ti during processing. From this point of view, processing technologies and/or parameters that imply a low decomposition degree of HA are very interesting for the end application. Shishkovsky *et al.* (2001) have found that the selective laser sintering (SLS) of NiTi-HA (4:1) powder mixtures led to more bioactive structures than in the case of furnace processing, as a consequence of the high heating rate of the material.

Although biocomposites with about 10 vol.% HA added to Ti powder proved to have the best biocompatibility and strength, compositions with larger amount of HA were often reported in the literature, as the mechanisms of phase formation represented the goal of the studies.

The current issue and full text archive of this journal is available at www.emeraldinsight.com/1355-2546.htm



Rapid Prototyping Journal
20/4 (2014) 301–310
© Emerald Group Publishing Limited [ISSN 1355-2546]
[DOI 10.1108/RPJ-09-2012-0083]

The authors acknowledge the project “Progress and development through post-doctoral research and innovation in engineering and applied sciences-PRIDE-Contract no. POSDRU/89/1.5/S/57083”, project co-funded from the European Social Fund through Sectorial Operational Program Human Resources 2007-2013.

Received 25 September 2012

Revised 7 February 2013

Accepted 22 April 2013

Limited data could be found in the literature referring to the manufacturing behaviour and final properties of Ti–HA biocomposites with a low HA amount, up to 5 vol.%, processed by selective laser melting (SLM).

The aim of this research work is to obtain medical-grade Ti6Al7Nb–HA biocomposites with a low amount of HA addition (2 and 5 vol.%) by means of SLM technique and to study them from a structural point of view.

2. Materials and methods

Atomized Ti6Al7Nb powder (MCP HEK GmbH), medical-grade, aimed for SLM applications and surface-conditioned (Marcu *et al.*, 2012), was used as base material.

HA was synthesized by the wet chemical precipitation method, at room temperature, using as reagents calcium nitrate tetrahydrate ($\text{Ca}(\text{NO}_3)_2 \cdot 4\text{H}_2\text{O}$) and diammonium hydrogen phosphate ($(\text{NH}_4)_2\text{HPO}_4$) (Sigma Aldrich), mixed as to obtain a molar ratio Ca/P equal to 1.67.

The mean particle size of Ti6Al7Nb and HA powders was 36 μm and inferior to 1 μm , respectively, as determined with a particle size analyser, Analysette 22 (Nanotec).

Two different mixtures of surface-conditioned Ti6Al7Nb powder with 2 and 5 vol.% HA were manually prepared. HA powder could not have been incorporated homogeneously in the base Ti alloy; some amount, mostly agglomerated particles, kept flowing on the top of the powder bed.

The flow rate of powders with and without HA additions was determined with a Carney funnel (5-mm-diameter orifice) flow meter.

The powders with and without HA, as reference material, were used as feeding materials for an MCP Realizer machine (MCP) with an Nd:YAG (fiber laser) and a maximum laser power of 200 W. Test specimens with dimensions of $10 \times 5 \times 3 \text{ mm}^3$ were manufactured under the following conditions:

- laser power: 50 W, 70 W, 100 W, 160 W, 180 W and 200 W;
- laser spot size: 150 μm ;
- layer thickness: 50 μm ;
- hatch spacing: 100 μm ; and
- scan speed: 400 mm/s.

The same building strategy was used for all produced samples; the successive layers being deposited in the “z” direction. The manufacturing process was performed in an argon atmosphere to prevent oxidation. The samples were built on a titanium plate whose temperature was kept at approximately 200°C for minimizing the thermal gradients during the process.

The manufactured samples were cleaned ultrasonically in distilled water for 10 min, and then dried at 80°C for 30 minutes.

Oxygen analyses were carried out with LECO TC400 equipment, based on the gas fusion principle. The sample mass was 0.1 mg.

Density, total porosity and open porosity were measured by Archimedes’ method, as according to ISO 2738. Weight measurements were performed with an XT 220A Precisa balance at an accuracy of 0.0001 g. The reported values represent the average of two measurements.

Metallographic samples were prepared as according to the standard procedure. Etching was performed with Kroll’s

reagent. The microstructure related to cross-section (along the “z” building direction), and “x-y” scanning plane (perpendicular to “z” building direction) of the SLM specimens was characterized by optical microscopy with the help of an Olympus GX51 optical microscope and scanning electron microscopy (SEM) using a Philips XL30 ESEM equipped with a sapphire Si(Li) EDS detector.

Microhardness measurements were carried out on unetched metallographic surfaces with the help of a Paar MHT-4 tester, by applying a load of 1N. Five measurements for each microstructural constituent and/or area with a similar microstructure were averaged.

3. Results and discussion

3.1 Oxygen analysis

The oxygen content of as received (not surface-conditioned) Ti6Al7Nb powder was 0.22 wt.%, while after the surface conditioning treatment, it was found equal to 0.55 wt.%. After SLM processing, 0.63 wt.% and 0.60 wt.% oxygen were measured in samples manufactured with 50 W and 200 W, respectively, indicating that the oxygen pick-up does not depend on the laser power but mainly on the oxygen content of the initial powder (Zhang *et al.*, 2011). Samples with HA were not subjected to this analysis because, due to the presence of oxygen in the HA structure, the results would have been irrelevant.

3.2 Flow behaviour

Flow rate values of powders with and without HA addition are given in Table I. It results that flowability slightly decreases by increasing the amount of HA, probably due to the presence of water adsorbed on the surface of HA particles. It should be specified that the manufacturing process was not affected by the impaired powder flow behaviour.

3.3 Density and porosity

The density and the total and open porosity values of the studied biocomposites with different HA additions and different applied laser powers are reported in Table II. By increasing the laser power, all materials display an increase of density and a decrease of total and open porosity. The values of open and total porosity are quite close, suggesting that the pores are mainly interconnected, which is positive, as it ensures the viability of the vascular system related to the future implant (Reis de Vasconcellos *et al.*, 2010).

3.4 Surface morphology

SEM images of surface morphology for SLM parts with 2 vol.% HA processed with 50, 70 and 100 W are shown as examples in Figure 1. Irrespectively to the amount of added HA, materials manufactured with lower laser powers as 50 and 70 W exhibited irregular surface morphologies, which facilitate the mechanical

Table I Flow rate of the studied powder mixtures

Material	Flow rate(s)
Ti6Al7Nb surface-conditioned	7.0
Ti6Al7Nb surface-conditioned with 2 vol.% HA	7.4
Ti6Al7Nb surface-conditioned with 5 vol.% HA	8.0

Table II Density and porosity values of studied materials

Laser power W	Material	Density g/cc	Total porosity (per cent)	Open porosity (per cent)
50	Ti6Al7Nb	3.50 ± 0.04	23 ± 2	21 ± 1
	Ti6Al7Nb with 2 vol.% HA	3.53 ± 0.02	22 ± 0	21 ± 0
	Ti6Al7Nb with 5 vol.% HA	3.50 ± 0.02	23 ± 5	22 ± 3
70	Ti6Al7Nb	3.68 ± 0.06	19 ± 1	18 ± 2
	Ti6Al7Nb with 2 vol.% HA	3.75 ± 0.12	17 ± 3	15 ± 3
	Ti6Al7Nb with 5 vol.% HA	3.80 ± 0.07	16 ± 3	15 ± 3
100	Ti6Al7Nb	4.13 ± 0.05	9 ± 32	6 ± 2
	Ti6Al7Nb with 2 vol.% HA	4.14 ± 0.05	9 ± 1	6 ± 2
	Ti6Al7Nb with 5 vol.% HA	3.97 ± 0.05	11 ± 3	10 ± 2
160	Ti6Al7Nb	4.15 ± 0.01	8 ± 0	7 ± 1
	Ti6Al7Nb with 2 vol.% HA	4.16 ± 0.08	8 ± 3	7 ± 3
	Ti6Al7Nb with 5 vol.% HA	4.13 ± 0.05	9 ± 1	7 ± 2
180	Ti6Al7Nb	4.22 ± 0.01	7 ± 0	7 ± 1
	Ti6Al7Nb with 2 vol.% HA	4.25 ± 0.08	6 ± 2	6 ± 1
	Ti6Al7Nb with 5 vol.% HA	4.28 ± 0.08	5 ± 2	3 ± 1
200	Ti6Al7Nb	4.26 ± 0.09	7 ± 0	6 ± 2
	Ti6Al7Nb with 2 vol.% HA	4.31 ± 0.06	5 ± 1	5 ± 3
	Ti6Al7Nb with 5 vol.% HA	4.37 ± 0.07	4 ± 1	3 ± 1

anchorage of the future implant (Sobieszczyk, 2010). As the laser power increased, the sample's surface became smoother, displaying the typical continuous scan tracks for SLM-processed Ti parts. The presence of the small-sized balls could be attributed to an eventual "balling" effect. The occurrence of small metallic balls on the surface of SLM-processed commercially pure Ti can be attributed to the instability of the liquid during the SLM processing as a consequence of the combination between material properties and process parameters (Gu *et al.*, 2012).

The BSE observations made at a slightly higher magnification evidenced the presence of some grey areas on the top surfaces of the same samples, indicated by arrows in Figure 2, which contained, besides Ti, Nb and Al of the base material, Ca and P, as resulted from energy-dispersive spectroscopy (EDS) analysis.

3.5 Analysis of bulk material

3.5.1 Fracture surfaces

The surfaces resulted by breaking the SLM-manufactured specimens along the building direction were analysed by SEM (SE and BSE mode) and EDS. Figure 3 shows the SEM–BSE image for the surface of a bulk pore positioned on the fracture surface of Ti6Al7Nb with 5 vol.% HA, SLM with 50 W. The presence of small, irregular particles stuck on the surface of the initial particles of the base powder could be noticed. As resulting from BSE observations, Figure 3b, the irregular particles are surrounded by dark grey areas with different extents. With respect to their appearance and qualitative chemical composition, the dark grey areas are very similar to those found on the top surfaces of SLM specimens, illustrated by Figure 2.

In samples with the same HA amount but obtained with an increased laser power, similar layers and/or compounds, with a dark grey appearance, covered the initial Ti alloy powder particles, as shown in Figures 4 and 5 for specimens processed with 100 and 200 W, respectively. In specimens of Ti–HA

processed by powder metallurgy, the presence of a compact layer on the surface of original Ti particles, consisting in a mixture of Ti_xP_y and $CaTiO_3$ phases, could be observed (Balbinotti *et al.*, 2011).

SEM–EDS measurements results and spot analyses, made on SLM specimens with 5 vol.% HA manufactured with 50, 100 and 200 W, are summarized in Table III. In a rough estimation, the atomic ratio Ca/P related to the layer formed on the surface of the initial Ti particles (surface of the bulk pores) of the investigated samples varied between 5.7 and 6.4. The ratio Ca/P resulted always higher than 1.67 corresponding to HA.

It could be therefore supposed that even if manufacturing time was very short, a certain amount of HA decomposed and interacted with the base material. On the other side, Shishkovsky *et al.* (2001) have shown that during high-velocity SLS processing, HA did not exhibit a strong decomposition in the NiTi–HA system.

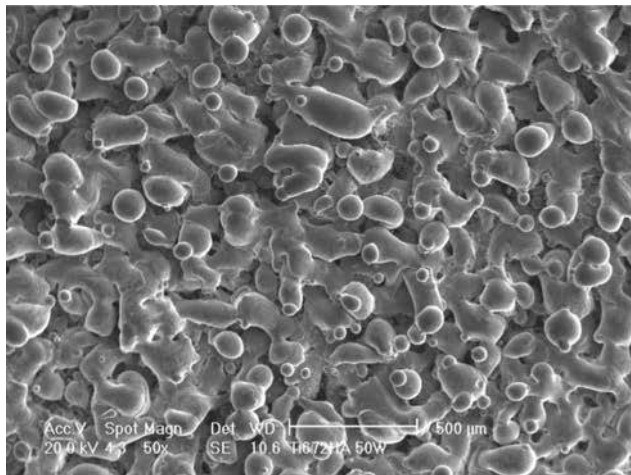
From the data reported in Table III, it results that the amounts of Ca and P measured on the surface of the bulk pores of the SLM-processed specimens decreased by increasing the laser power. Even more, samples manufactured with 50 W display clearly higher Ca and P amounts if compared to specimens processed with higher laser powers of 100 and 200 W. It is well-known that an increased laser power, and therefore input energy, determines a higher temperature during the process. Under a high laser energy input, the evaporation of the exposed powders may occur. It is, therefore, supposed that laser powers higher than 160 W are by far too high for materials considered in this study.

3.5.2 Microstructure

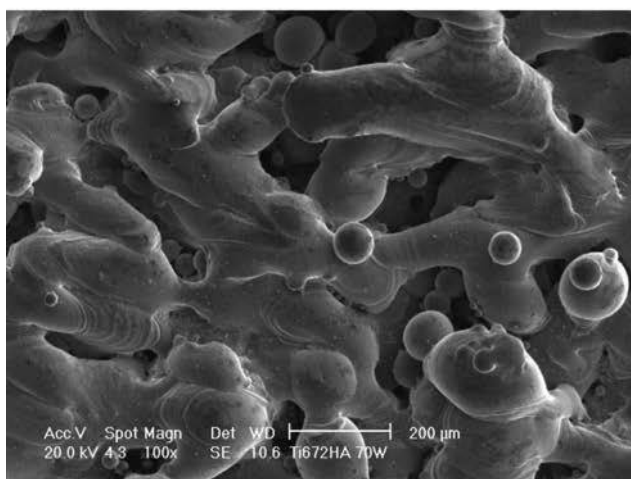
The microstructural features related to the "z" axis (building direction) and "x-y" plane (scanning plane) were both characterized for all studied materials.

In specimens obtained with a low laser power, pores were irregular along the building direction, as illustrated in Figure 6

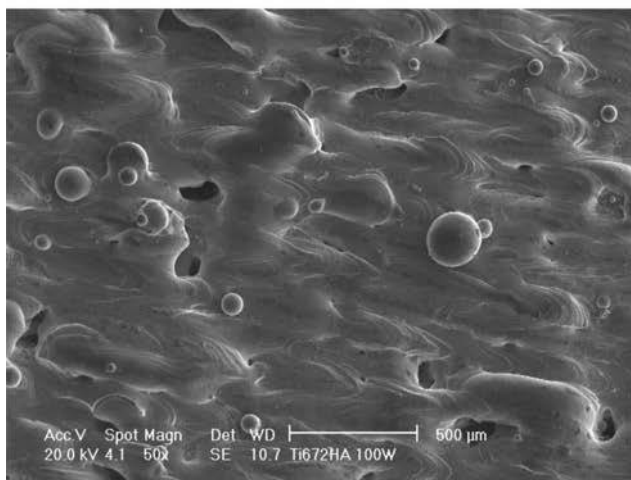
Figure 1 SEM image of surface morphology (top view) of Ti6Al7Nb with 2 vol.% HA specimens manufactured with (a) 50 W; (b) 70 W; (c) 100 W



(a)

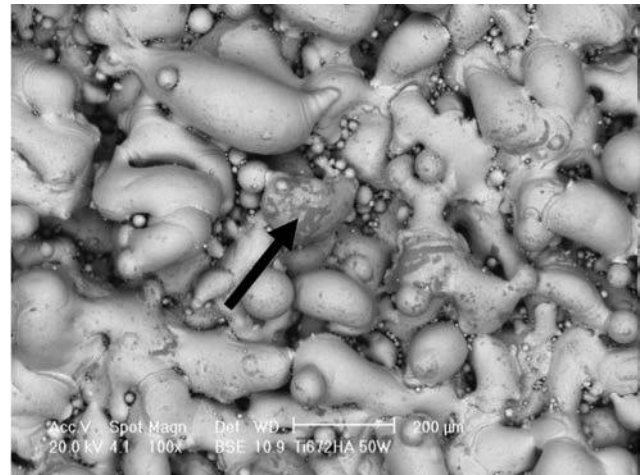


(b)

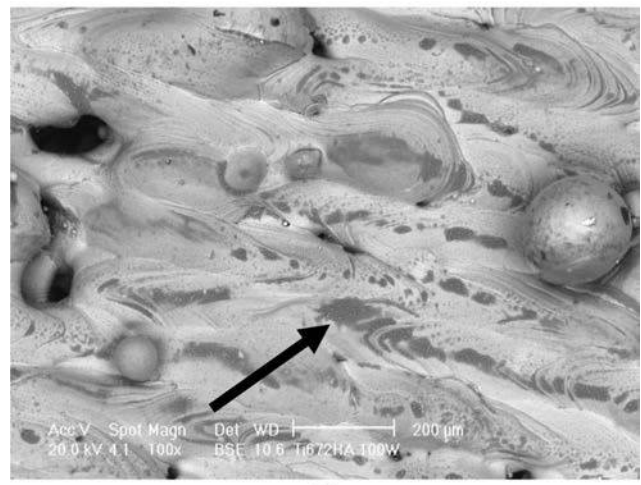


(c)

Figure 2 SEM–BSE image of surface morphology (top view) of Ti6Al7Nb with 2 vol.% HA specimens manufactured with (a) 50 W; (b) 100 W



(a)



(b)

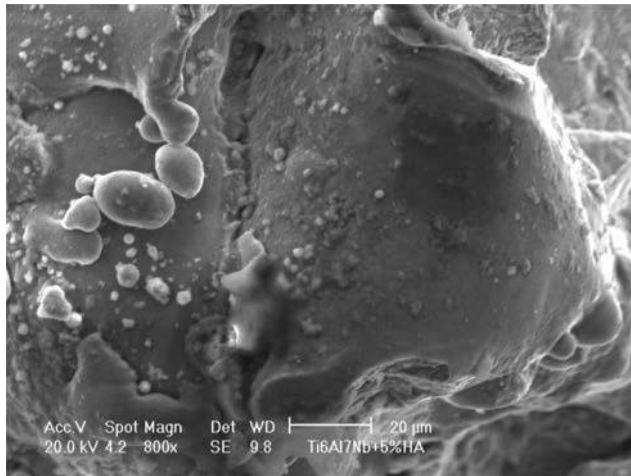
for Ti6Al7Nb manufactured with 70 W. Their amount decreased by increasing the applied laser power, supporting the results of density measurements.

After etching, all specimens displayed the typical SLM “band structure”, consisting in alternating white and dark bands, with columnar grains oriented along the z-axis, as shown in Figure 7. The matrix microstructure was mainly α' martensite (Marcu *et al.*, 2012). Samples manufactured with higher laser powers displayed narrow crack-like pores, indicated in Figure 7, possibly caused by the residual thermal stresses (Gu *et al.*, 2012).

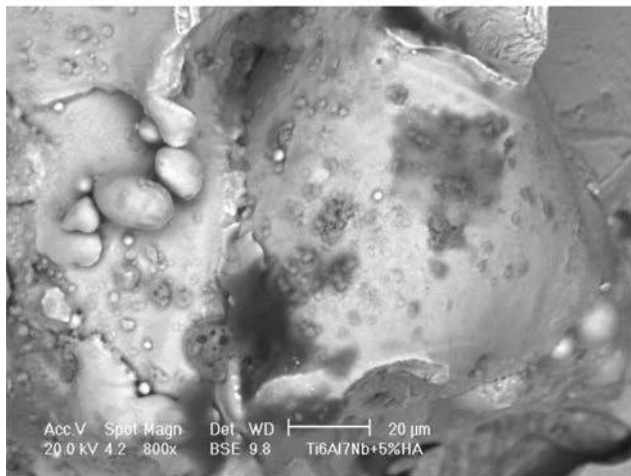
The dark bands were more sensitive to chemical etching, possibly due to the presence of small precipitates in the martensitic matrix. The related area is indicated by letter A in Figure 8.

A smaller grain size characterized materials with HA, Figure 9, as compared to that of reference materials, Figure 7, due, presumably, to a higher number of crystallization nuclei, e.g. unsolved oxides particles, in the melt (Hao *et al.*, 2009).

Figure 3 SEM–BSE image of the surface of a bulk pore on the fracture surface of Ti6Al7Nb with 5 vol.% HA manufactured with 50 W: (a) Secondary electrons (SE) image; (b) Back-scattered electrons (BSE) image



(a)



(b)

Figure 4 BSE image of a bulk pore in Ti6Al7Nb with 5 vol.% HA manufactured with 100 W

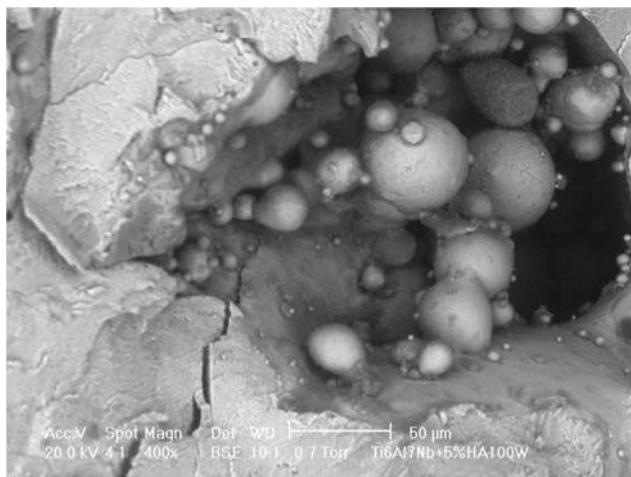


Figure 5 BSE image of a crack-like pore in Ti6Al7Nb with 5 vol.% HA manufactured with 200 W

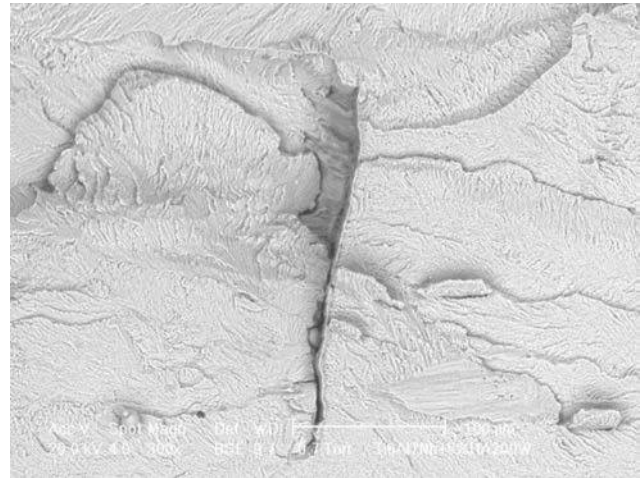
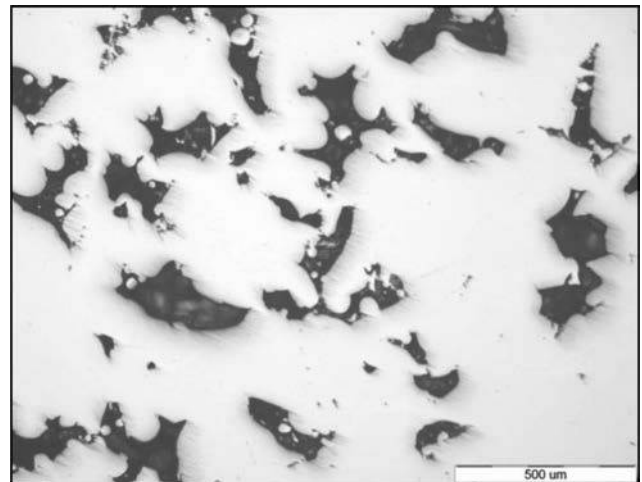


Table III Results of the EDS analyses made on the fracture surfaces of Ti6Al7Nb with 5 vol.% HA, SLM-processed with 50, 100 and 200 W

Material	Laser power W	Ca at. %	P at. %	Ratio Ca/P
Ti6Al7Nb with 5 vol.% HA	50	26.6	4.5	5.9
	100	5.1	0.8	6.4
	200	3.4	0.6	5.7

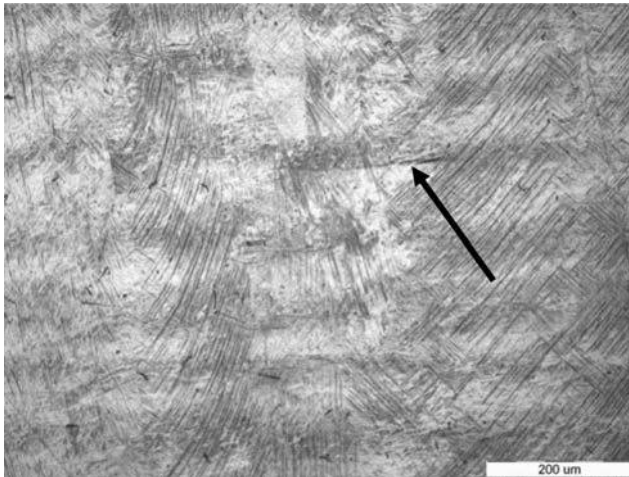
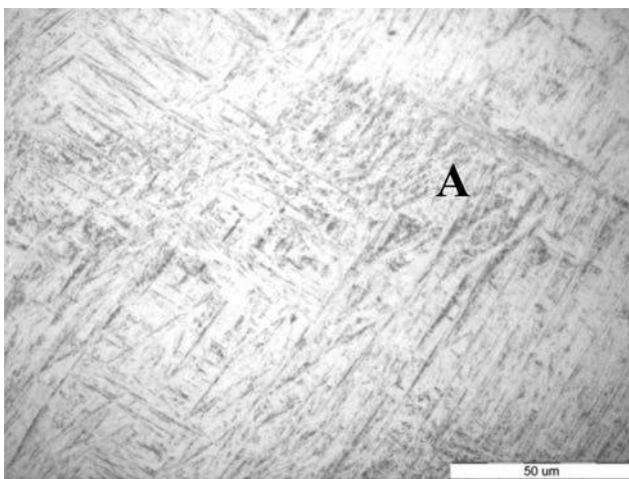
Figure 6 Pore morphology in SLM-processed Ti6Al7Nb, 70 W, unetched



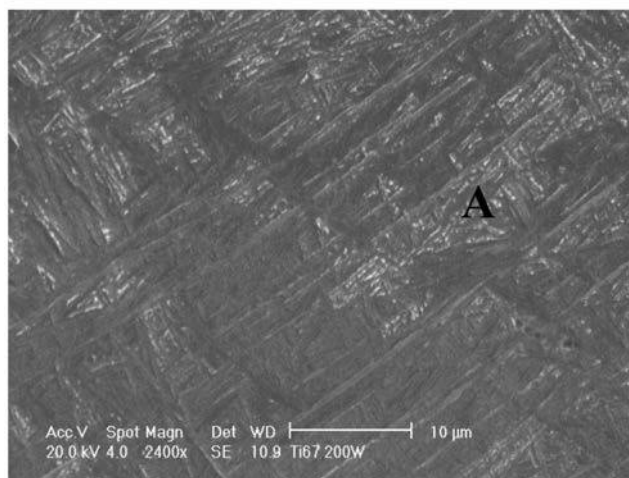
In HA-containing materials, besides the fine precipitates in the dark bands, area A in [Figure 10](#), a different microstructural feature was revealed, indicated by letter B in the same [Figure 10](#).

It appeared even darker than the typical SLM bands, with dense and very fine precipitates inside, as illustrated in [Figure 11](#), being positioned almost always in the vicinity of pores.

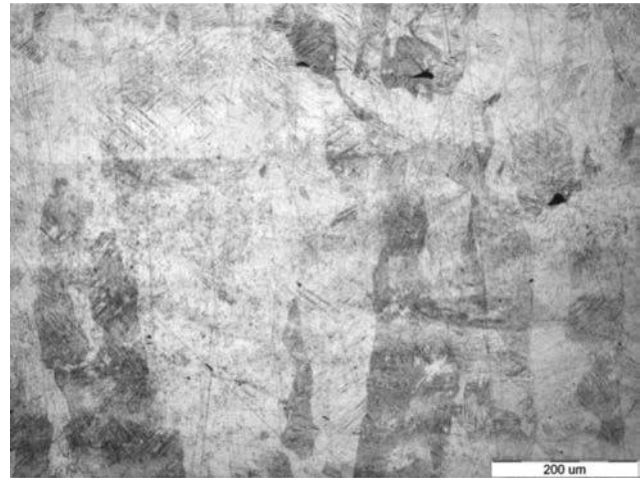
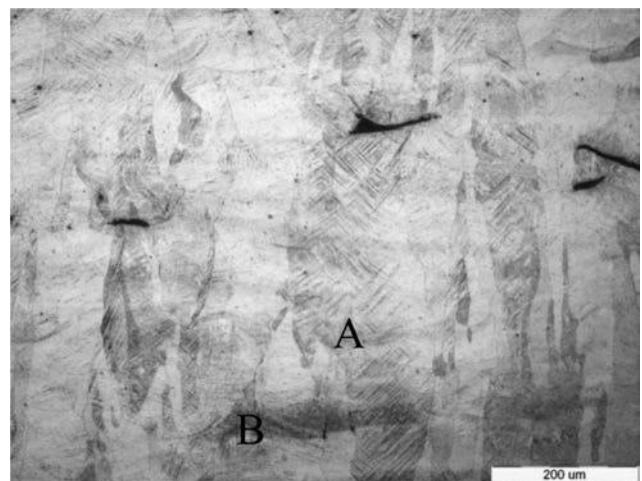
[Figure 12](#) illustrates the SEM image of “B” area in materials with 2 and 5 vol.% HA processed with 50 and 70 W, respectively. In materials with 2 vol.% HA, “B” area could be

Figure 7 Microstructure of Ti6Al7Nb processed with 200 W**Figure 8** Aspect of precipitates in “A” area in Ti6Al7Nb manufactured with 200 W

(a)



(b)

Notes: (a) Optical microscope image; (b) SEM image**Figure 9** Microstructure of Ti6Al7Nb with 2 vol.% HA manufactured with 200 W**Figure 10** Microstructure of Ti6Al7Nb with 2 vol.% HA manufactured with 160 W

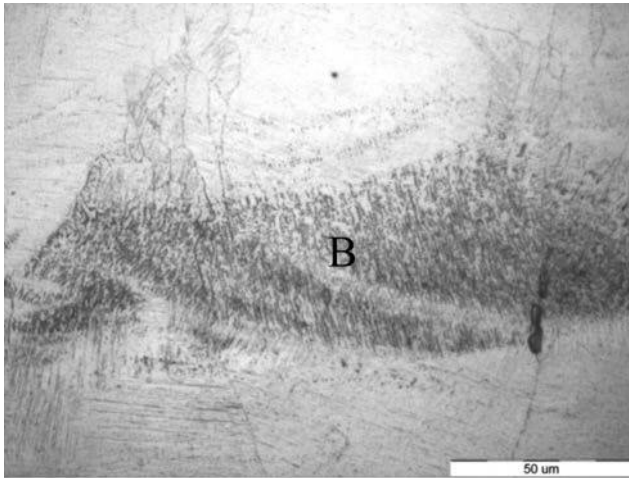
rather seen on the polished top and side surfaces of the specimens than in the polished cross-section. Specimens with 5 vol.% HA had more areas of the kind, both in the polished cross-section and on the polished top and side surfaces.

As displayed by the microstructure of polished top surface, parallel to the “x-y” scanning plane, [Figure 13](#), the pores are more rounded than along the “z” building direction. Grains are equiaxed in all studied materials, smaller in specimens with HA than in materials without HA, [Figure 14](#).

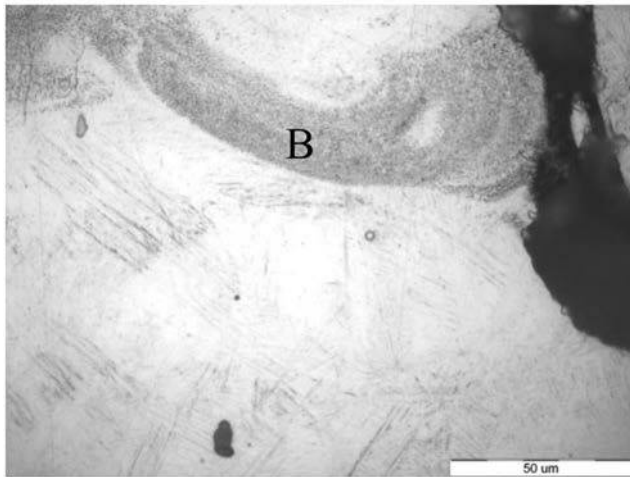
It could be, therefore, claimed that the microstructures of the SLM-processed Ti alloy–HA biocomposites are anisotropic, reflecting the layer-by-layer manufacturing strategy, as assessed by other authors ([Chlebus et al., 2011](#)).

Ti alloy–HA interaction during the SLM process was primarily evaluated through the microstructure of the manufactured materials. More detailed analyses were conducted on metallographic samples by means of SEM–BSE–EDS. It should be also specified that similar microstructures were investigated by X-ray diffraction (XRD) in a previous research ([Marcu et al., 2012](#)). The diffraction

Figure 11 Microstructure of Ti6Al7Nb with 2 vol.% HA manufactured with (a) 160 W; (b) 100 W



(a)



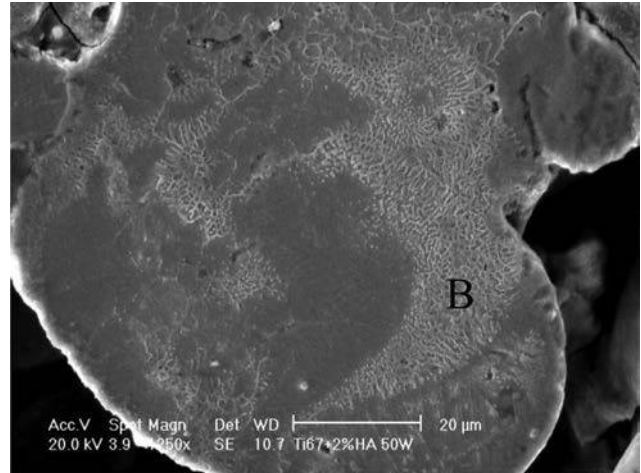
(b)

patterns related to the top surface of SLM specimens, as processed and polished, and to the polished cross-section (along the building direction) displayed only the reflections of hcp Ti. However, when XRD analyses were used for analysing similar materials with low HA additions, the high amount of Ti and/or Ti oxides would shadow the peaks of HA and calcium phosphates, which could limit the accuracy of the result. From the other side, the peaks of HA and different calcium phosphates are very close to each other or overlap, making the reading quite difficult (Ye *et al.*, 2009).

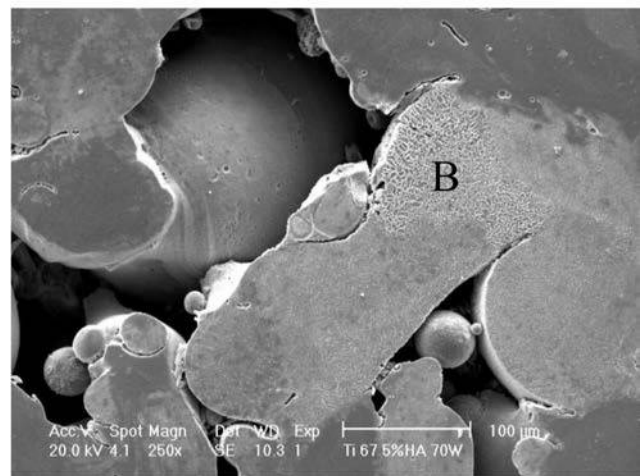
SEM-EDS analysis revealed the presence of P in the martensitic matrix (white bands), on the polished cross-section surfaces of specimens with 2 and 5 vol.% HA, in amount of 0.8 at.% and slightly superior to 1 at.%, respectively. No traces of Ca were found. By increasing the laser power, a slightly higher amount of P was measured in the martensite (white bands).

Considering that P has a small atomic radius, this could be the result of P diffusion into Ti alloy particles during SLM processing.

Figure 12 SEM image of “B” area in (a) Ti6Al7Nb with 2 vol.% HA manufactured with 50 W; (b) Ti6Al7Nb with 5 vol.% HA manufactured with 70 W



(a)



(b)

Figure 13 Microstructure of Ti6Al7Nb with 2 vol.% HA manufactured with 100 W; section parallel to the “x-y” scanning plan

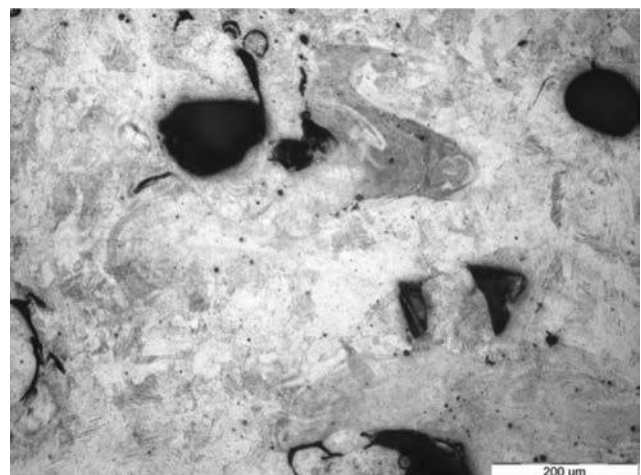
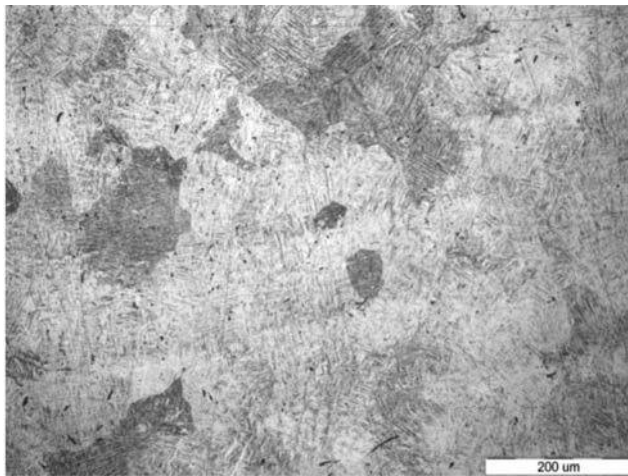
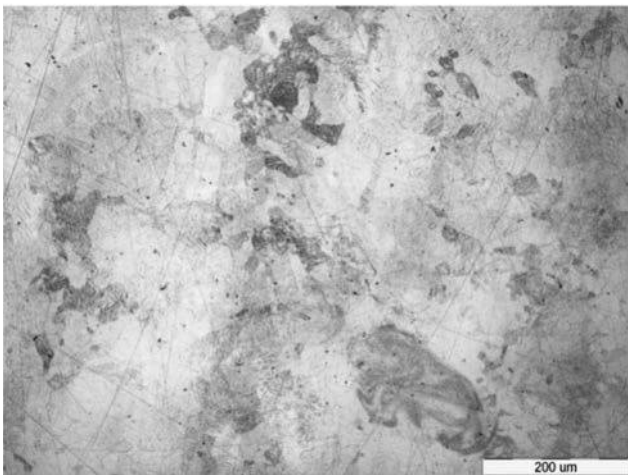


Figure 14 Microstructure of specimens manufactured with 200 W, section parallel to the “x-y” scanning plan



(a)



(b)

Notes: (a) Ti6Al7Nb; (b) Ti6Al7Nb with 2 vol.% HA

A P amount ranging between 1 and 3 at.% was measured by EDS spot analysis in “A” area, with fine precipitates. Ca was not detected here, irrespectively to the HA amount and laser power. Even if P appeared to be present in a higher amount in the bands with precipitates (“A” area/dark bands) than in the matrix (white bands), this result is not relevant. The difference between the P amount detected in the white and black bands could be attributed to many factors as initial amount, homogeneity and type of the P-containing compound in the analysed volume. It should be specified that EDS were made by spot analysis for a 1,500× magnification.

A maximum of 3 at.% of P was detected by spot analysis in “B” area of HA-containing materials. Ca was found only in materials processed with 50 W, in an amount of 1.5 at.% approximately.

3.5.3 Microhardness

For a better understanding and evaluation of the microstructure, HV0.1 microhardness of all studied materials

was measured on the three different microstructural features, α' martensite (white bands), “A” area (dark bands) and “B” area, the last being found only in the materials with HA addition.

The values for Ti6Al7Nb given in Figure 15 indicate that the microhardness of the alternating white and black bands occurring in the microstructure of the sample cross-section (along the “z” building direction) is very similar, irrespectively to the used laser power. In samples containing HA, the microhardness of “A” area remained close to that of the white band. A higher microhardness was measured on “B” area, of about 650 and 700 HV0.1 in samples containing 2 and 5 vol.% HA, respectively. Some microcracks were found in some of these regions. It could be assessed that the occurrence of “B” area embrittled the material.

Figure 16 reports the microhardness of α' martensite (white bands) in materials with 2 and 5 vol.% HA and without HA, processed with different laser powers. It results that the microhardness increased with the amount of HA added to the base Ti alloy powder, due to the smaller grain size and increased amount of P diffused in the bulk of formerly HA-containing specimens.

For the same HA amount, the metallic bulk of specimens processed with 50 W has a lower microhardness than that of specimens manufactured with higher laser powers, Figure 16.

Figure 15 Microhardness of white and dark bands in SLM-processed Ti6Al7Nb

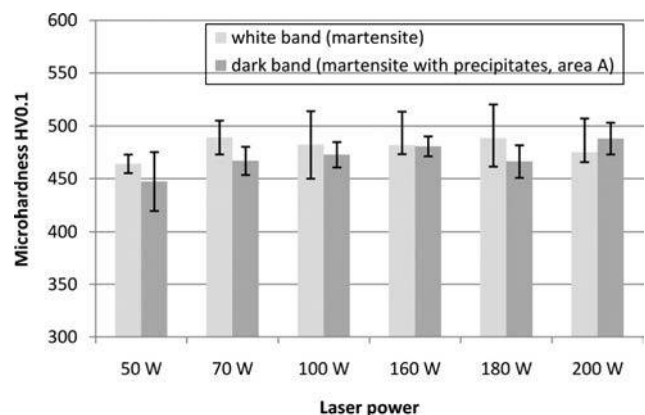
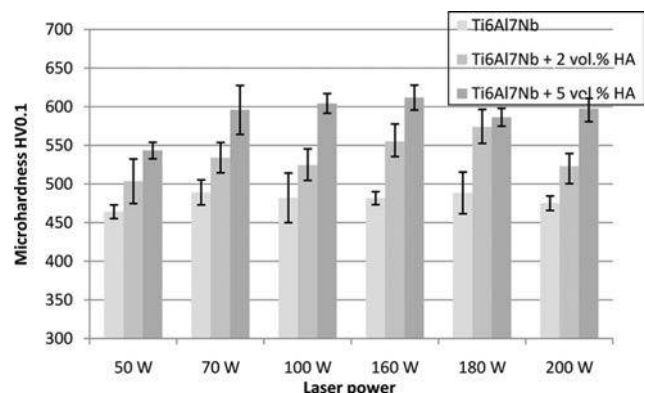


Figure 16 Microhardness of α' martensite in white bands of materials with different amounts of HA



On the other side, only in samples processed with 50 W (polished section), both Ca and P were detected by EDS. Those are indications of the fact that in materials manufactured with 50 W, the degree of decomposition and/or interaction with of HA Ti powder were lower compared to the higher laser powers.

The future research aims to assess the biocompatibility of the SLM-processed biocomposites.

The research was carried out within the BIOMAPIM project, financed by the Romanian National Council for the Higher Education Scientific Research.

4. Conclusions

1. The addition of 2 and 5 vol.% HA powder to medical-grade, surface-conditioned Ti6Al7Nb powder slightly impaired the flow behaviour of the base material.
2. The density of manufactured SLM specimens, with and without HA, increased together with the applied laser power.
3. The HA-containing materials displayed decomposition compounds on the top and side surfaces of the SLM-manufactured specimens.
4. In the materials processed with lower laser powers, e.g. 50 W, the decomposition and/or interaction compounds of HA with Ti6Al7Nb base powder were found on the surface of the bulk pores, covering at a different extent the surfaces of the original Ti alloy powder particles.
5. The microstructure of SLM specimens with and without HA is anisotropic: the polished surfaces exhibited columnar grains along the “z” building direction and equiaxed grains in the “x-y” scanning plane. The typical band structure of SLM-manufactured parts characterized the produced biocomposites. The microstructure of all studied materials displayed mainly α' martensite, irrespectively to the applied laser power. Finely dispersed secondary phases precipitated in the martensitic matrix during processing were found in dark bands. In Ti6Al7Nb, these did not have any significant impact on the microhardness, irrespectively to the used laser power.
6. A smaller grain size characterized the SLM-manufactured materials with HA addition, if compared to the materials without HA.
7. The degree of decomposition and interaction of HA with the base Ti6Al7Nb powder depended on the applied laser power and initial HA amount.
8. In the polished section, the microstructure of HA-containing materials displayed, besides α' martensite and finely dispersed precipitates, very similar to those seen in the dark bands of SLM-processed Ti6Al7Nb, a third microstructural feature which is directly related to the interaction Ti-HA, where Ca was sometimes detected together with P. The microhardness of the related areas was of about 700 HV 0.1.

P was found overall in the microstructure, in a higher amount in areas with precipitates (dark band) than in the martensitic matrix (white band). Although not evidenced by the investigation techniques used in this research work, the presence of Ti_xP_y -type phase in the structure of studied biocomposites was assumed.

9. The microhardness of α' martensite increased with the amount of added HA from about 480 HV0.1 in Ti6Al7Nb to 536 HV0.1 in Ti6Al7Nb with 2 vol.% HA and further to 590 HV 0.1 in Ti6Al7Nb with 5 vol.% HA. The materials processed with 50 W had the lowest microhardness, due to a lower interaction of HA with the base powder.
10. The biocomposites processed with 50 W are the most promising for endosseous applications, with regard to pores volume/morphology and microstructure. The lower interaction of HA with the base Ti6Al7Nb as well as the mode of distribution of HA and/or decomposition products in the bulk and surface pores are beneficial for implant osseointegration. The presence of some remaining HA, likely dehydroxylated, with a disordered structure, in the SLM-manufactured specimen, might be possible.

References

- Balbinotti, P., Gemelli, E., Buerger, G., Amin de Lima, S., de Jesus, J. and Camargo, N.H.A. (2011), “Microstructure development on sintered Ti/HA biocomposites produced by powder metallurgy”, *Materials Research*, Vol. 14 No. 3, pp. 384–393.
- Bremen, S., Meiners, W. and Diatlov, A. (2012), “Selective laser melting: a manufacturing technology for the future?”, *Laser Technik Journal*, Vol. 9 No. 2, pp. 33–38.
- Chlebus, E., Kuznika, B., Kurzynowski, T. and Dybala, B. (2011), “Microstructure and mechanical behaviour of Ti-6Al-7Nb alloy produced by selective laser melting”, *Materials Characterization*, Vol. 62 No. 5, pp. 485–495.
- Gu, D., Hagedorn, Y.C., Meiners, W., Meng, G., Batista, R.J.S. and Wissenbach, K. (2012), “Densification behaviour, microstructure evolution and wear performance of selective laser melting processed commercially pure titanium”, *Acta Materialia*, Vol. 60 No. 9, pp. 3849–3860.
- Hao, L., Dadbakhsh, S., Seaman, O. and Felstead, M. (2009), “Selective laser melting of a stainless steel and hydroxyapatite composite for load-bearing implant development”, *Journal of Materials Processing Technology*, Vol. 209 No. 17, pp. 5793–5801.
- Marcu, T., Todea, M., Gligor, I., Berce, P. and Popa, C. (2012), “Effect of surface conditioning on the flowability of Ti6Al7Nb powder for selective laser melting applications”, *Applied Surface Science*, Vol. 258 No. 7, pp. 3276–3282.
- Ning, C.Q. and Zhou, Y. (2002), “In vitro bioactivity of a biocomposite fabricated from HA and Ti powders by powder metallurgy method”, *Biomaterials*, Vol. 23 No. 14, pp. 2909–2915.
- Reis de Vasconcellos, L.M., Oliveira Leite, D., Nascimento de Oliveira, F., Rodarte Carvalho, Z. and Alves Cairo, C.A. (2010), “Evaluation of bone ingrowth into porous titanium implant: histomorphometric analysis in rabbits”, *Brazilian Oral Research*, Vol. 24 No. 4, pp. 399–405.
- Shishkovsky, I.V., Tarasova, E. Yu, Zhuravel, L.V. and Petrov, A.L. (2001), “The synthesis of a biocomposite based on nickel titanium and hydroxyapatite under selective laser sintering conditions”, *Technical Physics Letters*, Vol. 27 No. 3, pp. 211–213.

- Simchi, A. (2006), “Direct laser sintering of metal powders: mechanism, kinetics and microstructural features”, *Materials Science and Engineering A*, Vol. 428, pp. 148-158.
- Sobieszczyk, S. (2010), “Optimal features of porosity of Ti alloys considering their bioactivity and mechanical properties”, *Advanced in Materials Science*, Vol. 10 No. 2, pp. 20-30.
- Ye, H., Liu, X.Y. and Hong, H. (2009), “Characterization of sintered titanium/hydroxyapatite biocomposite using FTIR spectroscopy”, *Journal of Materials Science: Materials in Medicine*, Vol. 20 No. 4, pp. 843-850.

- Zhang, L.C., Klemm, D., Eckert, J., Hao, Y.L. and Sercombe, T.B. (2011), “Manufacture by selective laser melting and mechanical behaviour of a biomedical Ti-24Nb-4Zr-8Sn alloy”, *Scripta Materialia*, Vol. 65 No. 1, pp. 21-24.

Corresponding author

Teodora Marcu can be contacted at: teodora.marcu@stm.utcluj.ro

This article has been cited by:

1. Changjun Han, Qian Wang, Bo Song, Wei Li, Qingsong Wei, Shifeng Wen, Jie Liu, Yusheng Shi. 2017. Microstructure and property evolutions of titanium/nano-hydroxyapatite composites in-situ prepared by selective laser melting. *Journal of the Mechanical Behavior of Biomedical Materials* **71**, 85-94. [[CrossRef](#)]
2. Karl Davidson, Sarat Singamneni. 2016. Selective Laser Melting of Duplex Stainless Steel Powders: An Investigation. *Materials and Manufacturing Processes* **31**:12, 1543-1555. [[CrossRef](#)]
3. Dan Leordean, S. A. Radu, D. Frățilă, P. Berce. 2015. Studies on design of customized orthopedic endoprostheses of titanium alloy manufactured by SLM. *The International Journal of Advanced Manufacturing Technology* **79**:5-8, 905-920. [[CrossRef](#)]